WAVE REFRACTION ACROSS A SHEARING CURRENT

Ivar G. Jonsson[1] and Ove Skovgaard[2]

ABSTRACT

Conservation of wave crests and wave action is introduced to yield the new wave length L_2 and new wave height H_2 as a wave train of plane incidence crosses a shearing current; refraction angle α_2 is determined by Snell's law. Input parameters are water depth h (assumed constant), absolute wave period T_a, angle of incidence α_1, current velocities U_1 and U_2 (see Fig 1), and initial wave height H_1. Solution domains are also given, analytically and graphically. The numerical results for L_1, L_2, α_2, and H_2 are presented non-dimensionally in a number of figures, with dimensionless input parameters. As a direct illustration of the effect of the shearing current, a sequence of graphs are presented, showing in dimensional form the variation of L_2, α_2, H_2, and steepness $S_2 = H_2/L_2$ with U_2 for fixed values of h, α_1, U_1, T_a, and H_1. Large positive and negative currents can increase the steepness significantly. The variation of S_2/S_1 with T_a and h is finally depicted, demonstrating the "filtering" effect of a shearing current on waves.

A numerical example shows how simple it is to calculate accurately quantities L_1, L_2, α_2, and H_2.

1. INTRODUCTION

The purpose of this study is to examine the transformation of waves advancing across a shear layer, from a region of current velocity U_1 to one of current velocity U_2, see Fig 1. Changes will occur in wave length and height, and in direction and speed of propagation. The results are presented in a number of graphs.

Studies of this kind were initiated by Longuet-Higgins and Stewart (1961), who considered the special case of deep water waves progressing from still water into a region with a steady, uniform current. Here we shall consider the general case of waves on an arbitrary (constant) depth, with arbitrary (steady and uniform) current velocities on both sides of the shear layer. Large-scale currents are considered, i e the current gradient is assumed small everywhere.

In region 1 we prescribe regular and plane incoming waves, and thus also the transmitted waves in region 2 will be plane. The two regions of flow are denoted by subscripts 1 and 2. In these regions current velocities are therefore specified as U_1 and U_2. Assuming linear theory, solutions are sought for wave lengths L_1 and L_2, refraction angle α_2 (see

---

[1] Associate Professor, Institute of Hydrodynamics and Hydraulic Engineering (ISVA), Bldg. 115, Technical University of Denmark, DK-2800 Lyngby.

[2] Associate Professor, Laboratory of Applied Mathematical Physics (LAMF), Bldg. 303, same address.
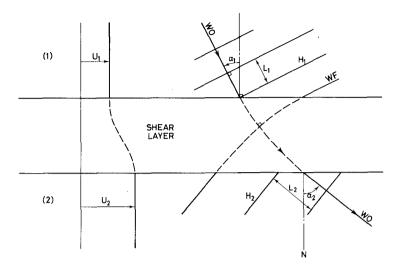
Fig 1. Waves advancing across a shearing current, from region 1
       to region 2. WF and WO mean wave front and wave orthogonal.
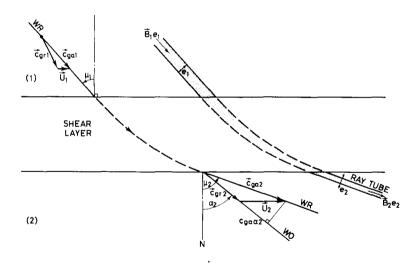   Horizontal sketch.

Fig 2. Wave ray WR and ray tube passing a shear layer, from re-
       gion 1 to region 2. Horizontal sketch.

Fig 1), and wave height H_2. Given values are water depth h, current velo-
cities U_1 and U_2, absolute wave period T_a, angle of incidence α_1 (see Fig
1), and incoming wave height H_1.

Velocities U are taken positive in the direction of wave travel. If we then consider only positive α-values, a positive (i e following) current is one running towards the right in Fig 1.

Since large-scale currents are assumed, reflection is excluded a priori, and the waves are purely progressive in both regions. This means in principle that the width of the shear layer must be several wave lengths. In practice this needs not be so, however. This can be seen from Evans (1975), who found transmission and reflection characteristics for a current discontinuity in deep water. He showed "that the amplitude of the transmitted wave as a function of the angle of incidence and current strength is very close to that obtained by Longuet-Higgins and Stewart [1961] on the assumption of small smooth changes in current velocity". This is not immediately expected, since in the former case the flow is not matched in detail at the discontinuity. Only for larger angles of incidence wave transmission was significantly affected by the no-reflection assumption. Reference is made to Evans' Fig 1 and Peregrine's (1976) Fig 12. So although the correct solution to the general problem has not been found yet (Peregrine, 1976, p 73), there is hope that the wave heights presented herein are good approximations also for narrow shear layers. (The only thing for certain is that the height found for the transmitted wave is too large).

We have also excluded the effect of turbulence generated by the shear layer. Here Evans (1975) concluded on the basis of Savitsky's (1970) investigations that turbulence thus generated will have a smaller influence than the mean velocity gradients in the flow. Another more important aspect (for narrow shear layers) is that they are unstable, so that steady solutions here cannot be expected to give more than somewhat crude approximations (Peregrine, 1976, p 71).

The current is assumed constant over depth. The effect of a possible vorticity was examined by Jonsson et al (1978). Dissipation is neglected, but can be included as described in Chapter 3.

The general case of current depth refraction has been studied elsewhere, see for instance Skovgaard and Jonsson (1977), Jonsson and Wang (1978), and the two review articles by the senior author (Jonsson, 1977, 1978b):

For completeness it is mentioned that fundamentally it is not a requirement that regions exist in which U_1 and U_2 are constant; the results obtained are in fact valid going from any point with current velocity U_1 to any other point with velocity U_2, the flow being parallel over a horizontal bed, and disregarding dissipation.

2.   SOME BASIC CONCEPTS

Since wave motion in a moving medium is so different from that in still water, it is worth while starting with the introduction of some concepts, which are important for this type of flow.

In each region we have two frames of reference. One is a coordinate system fixed on a plane earth, in which the wave period (T_a) is constant. This is the common absolute frame of reference, in which we use subscripts 'a'. The other is a Galilean transformation of the first where

the transformation velocity is the current velocity. Observations in the moving system(s) are referred to as relative, and subscripts 'r' are used here.

It is obvious that an important quantity as for instance the relative wave period is not the same in the two systems. The relation is found in the following way. Looking at Fig 1, it is seen that in the absolute frame, the wave front during time T_a has travelled distance

$$L = c_a T_a \tag{2.1}$$

where L is the wave length, and c is the phase speed (here absolute) of the wave. Seen from the moving observer the front has travelled distance $c_r T_a$ during the same time interval. At the same time, the observer him/herself has travelled distance UT_a in the current direction. By projecting this on the wave orthogonal, we hereafter find for the absolute phase speed, after having divided by T_a

$$c_a = c_r + U \sin \alpha \tag{2.2}$$

where α is the angle between the normal N to the streamlines and the wave orthogonal. Since we also by definition have

$$L = c_r T_r \tag{2.3}$$

we get from (2.1) and (2.2) for the relative period T_r

$$\frac{1}{T_r} = \frac{1}{T_a} - \frac{U \sin \alpha}{L} \tag{2.4}$$

It appears that for a following current ($U \sin \alpha > 0$) we have $T_r \gtrless T_a$, as expected. In the literature (2.4) is often written $\omega_r = \omega_a - \vec{k} \cdot \vec{U}$ ('conservation of wave crests'), where $\omega = 2\pi/T$, the angular frequency, and $\vec{k}$ is the wave number vector, which is a vector of magnitude $2\pi/L$ going in the wave orthogonal direction.

In Fig 1 α_1 is the angle of incidence and α_2 the refraction angle.

In current wave systems it is important to distinguish between three sets of curves: Streamlines, wave orthogonals, and wave rays. A streamline gives the (local) mean flow direction. A wave orthogonal is normal to the wave front, and gives the direction of wave travel. Finally a wave ray gives the direction of the absolute group velocity, i e of

$$\vec{c}_{ga} = \vec{c}_{gr} + \vec{U} \tag{2.5}$$

where the relative group velocity $\vec{c}_{gr}$ goes in the orthogonal direction, see Fig 1. Wave rays determine wave heights since the so-called wave action, defined as

$$\text{Wave action} \equiv \frac{E}{\omega_r} \tag{2.6}$$

is conserved along wave rays, see Chapter 3.

In (2.6) E is the specific wave energy

$$E = \frac{1}{8} \rho g\, H^2 \tag{2.7}$$

and ω_r is the relative angular frequency. In (2.7) ρ is density, g gravity acceleration, and H is the wave height.

The component of (2.5) in the direction of the orthogonal is also an important quantity. It is given by

$$c_{ga\alpha} = c_{gr} + U \sin \alpha \tag{2.8}$$

The complete differential equations for wave orthogonals and wave rays for a general system are presented in the Appendix.

3. THE GOVERNING EQUATIONS

Since linear theory is assumed, the relative phase speed is given by

$$c_r = \sqrt{\frac{g}{k} \tanh kh} \tag{3.1}$$

where $k = 2\pi/L$, the wave number, and h is the water depth. Similarly we have for the relative group speed

$$c_{gr} = \frac{1}{2} c_r (1 + G) \qquad (3.2) \qquad \text{with} \quad G \equiv \frac{2kh}{\sinh 2kh} \qquad (3.3)$$

REGION 1 – Wave length L_1 can be found by eliminating c_{a1} and c_{r1} from (2.1), (2.2), and (3.1). The (implicit) result is

$$\sqrt{\frac{h}{L_1} \tanh k_1 h} = \sqrt{\frac{h}{L_o}} \left[1 - \frac{U_1 \sin \alpha_1\, T_a}{L_1} \right] \tag{3.4}$$

in which $k_1 = 2\pi/L_1$, and L_o is the deep water wave length in the absence of currents, i e

$$L_o = \frac{g}{2\pi} T_a^2 \tag{3.5}$$

Equation (3.4) is identical with (3.5) in Jonsson et al (1971). In a dimensionless representation it gives L_1/L_o as a function of h/L_o and $U_1 \sin \alpha_1/c_o$, where c_o is the deep water phase speed in the absence of currents, i e

$$c_o = \frac{g}{2\pi} T_a \tag{3.6}$$

Solutions to (3.4) are depicted in Fig 6. Values of L_1/L_o can also be read in Tables 6-a and 6-b in Jonsson et al (1971), remembering that entry parameter q* there equals $(h/L_o)(U_1 \sin\alpha_1/c_o)$. Also Tables 3.2-I and 3.2-II in Jonsson (1978b) can be used.

REGION 2 – Equation (3.4) is valid for this region also, if subscript 1 is replaced by subscript 2. Inserting Snell's law

$$\frac{L_1}{\sin\alpha_1} = \frac{L_2}{\sin\alpha_2} \tag{3.7}$$

into the "new" (3.4) then yields for the determination of L_2

$$\sqrt{\frac{h}{L_2}\tanh k_2 h} = \sqrt{\frac{h}{L_o}}\left[1 - \frac{U_2\sin\alpha_1\ T_a}{L_1}\right] \tag{3.8}$$

in which $k_2 = 2\pi/L_2$, the wave number in region 2. This determines L_2/L_o as a function of h/L_o, $U_1\sin\alpha_1/c_o$, and $U_2\sin\alpha_1/c_o$. Solutions to (3.8) are depicted in Figs 7 - 10.

Note that (3.8) can be solved in quite another way than (3.4). Since we assume that L_1 has now been calculated, the right-hand side of (3.8) is known. Ratio h/L_2 can therefore be found from a conventional table for surface gravity waves (e g Wiegel, 1964, Appendix 1) using the square of the right-hand side of (3.8) as entry in the column "h/L_o". L_2 is here-after found as $h/(h/L)$; it cannot be found from $L = L_o\tanh kh$!

Refraction angle α_2 is determined from Snell's law as

$$\alpha_2 = \text{Arcsin}\ \frac{L_2\sin\alpha_1}{L_1} \tag{3.9}$$

This equation gives α_2 as a function of h/L_o, α_1, U_1/c_o, and U_2/c_o, as shown in Figs 11 - 26.

Wave height H_2 is found from wave action conservation. In the general case this principle reads, see Christoffersen and Jonsson (1979) and Jonsson (1978b)

$$\nabla\cdot\left(\frac{E}{\omega_r}\vec{c}_{ga}\right) + \frac{E_d - \vec{\tau}_b\cdot\vec{U}}{\omega_r} = 0 \tag{3.10}$$

where ∇ is the horizontal gradient operator $(\partial/\partial x, \partial/\partial y)$, E, and $\vec{c}_{ga}$ are given by (2.7) and (2.5), ω_r is the relative angular frequency, E_d is the dissipation per unit horizontal area, and $\vec{\tau}_b$ the (mean) bed shear stress (wind shear is neglected). It is repeated that E/ω_r is wave action. The wave action flux is often termed $\vec{B}$, i e

$$\vec{B} \equiv \frac{E}{\omega_r}\vec{c}_{ga} \tag{3.11}$$

A simple proof of the wave action conservation principle for irrota-tional flow has been given by the senior author, Jonsson (1978a). In Christoffersen and Jonsson (1979) the general expression (3.10) was de-duced.

In this study dissipation is neglected, and (3.10) reduces to $\nabla\cdot\vec{B} = 0$. Looking at the ray tube in Fig 2 we then find using Gauss' theorem

$$B_1 e_1 = B_2 e_2 \tag{3.12}$$

where $B = |\vec{B}|$ and e is the tube width. Thus we find for H_2, using (3.11) and (3.12)

$$\frac{H_2}{H_1} = \sqrt{\frac{\omega_{r2}}{\omega_{r1}}\frac{c_{ga1}}{c_{ga2}}}\frac{1}{\sqrt{\beta_r}} \tag{3.13}$$

where β_r is the <u>ray separation factor</u> $e_2/e_1 = \cos\mu_2/\cos\mu_1$; μ is the angle between the ray and the normal N in Fig 2. From this figure we also have $c_{ga} \cos\mu = c_{gr} \cos\alpha$. Introducing c_{gr} through (3.2) and further using that $c_r/\omega_r = 1/k$ and that $k_2/k_1 = \sin\alpha_1/\sin\alpha_2$ (Snell), we find from (3.13)

$$\frac{H_2}{H_1} = \sqrt{\frac{1 + G_1}{1 + G_2}} \sqrt{\frac{\sin 2\alpha_1}{\sin 2\alpha_2}} \qquad\qquad (3.14)$$

Equation (3.14) gives H_2/H_1 as a function of h/L_o, α_1, U_1/c_o, and U_2/c_o. It shows that in this approach H_2 is a linear function of H_1. The variation of H_2/H_1 is depicted in Figs 11 - 26. In deep water (G = 0) (3.14) reduces to Longuet-Higgins and Stewart's (1961) expression $H_2/H_1 = (\sin 2\alpha_1/\sin 2\alpha_2)^{\frac{1}{2}}$.

In the special case considered here, the wave height can also be found by a simple momentum consideration. The "shear stress" in a section parallel with the streamlines is according to Jonsson (1978a) or (1978b, Section 3.2.3.2) $F_m \sin\alpha \cos\alpha$, where $F_m = 1/16 \, \rho g H^2 (1 + G)$, the momentum part of the radiation stress. Since this "shear stress" must be the same on the two sides of the shear layer, (3.14) follows directly.

As α_2 approaches $90°$, H_2 goes towards infinity according to (3.14), and the theory breaks down. The physical situation is U_2 being so much larger than U_1 that the waves are "swept" along the "first" U_2 streamline, and wave orthogonals <u>and</u> rays run parallel with it. The ray separation factor then goes towards zero. In practice this will give a strong reflection, which is disregarded in the theory.

The wave steepness S_2 ($\equiv H_2/L_2$) is given both directly (Fig 30) and relative to S_1 (Fig 31), for one set of parameters.

MEAN WATER LEVELS - There will be a slight difference in mean water level between regions 1 and 2. Using the formulae in Jonsson (1978a) or (1978b, Section 3.2.3.2), equilibrium at right angles to the streamlines gives

$$\frac{1}{2} \rho g h_1^2 + F_{p1} + F_{m1} \cos^2\alpha_1 = \frac{1}{2} \rho g h_2^2 + F_{p2} + F_{m2} \cos^2\alpha_2 \qquad (3.15)$$

in which $F_p = 1/16 \, \rho g H^2 G$, the pressure part of the radiation stress, and F_m is the previously given momentum part. After some manipulations, hereunder using (3.14), we find for the difference in mean water level, defined as $b = h_2 - h_1$

$$b = \frac{H_1^2}{16h} G_1 \left[1 - \frac{G_2(1 + G_1)}{G_1(1 + G_2)} \frac{\sin 2\alpha_1}{\sin 2\alpha_2} + \frac{1 + G_1}{G_1} \frac{\cos\alpha_1}{\sin\alpha_2} \frac{\sin(\alpha_2 - \alpha_1)}{\sin\alpha_2} \right] \qquad (3.16)$$

correct to second order. Since the factor to the square bracket is recognized as the conventional wave set-down (over a varying bottom) it appears that b is indeed a small quantity, by order of magnitude 1 cm. For normal incidence ($\alpha_1 = 0°$), and in deep water, b vanishes.

4.   SOLUTION DOMAINS

REGION 1 - As shown by Jonsson et al (1971, p 493), there are no solutions to the wave length expression (3.4), if the wave orthogonal component $c_{ga\alpha}$
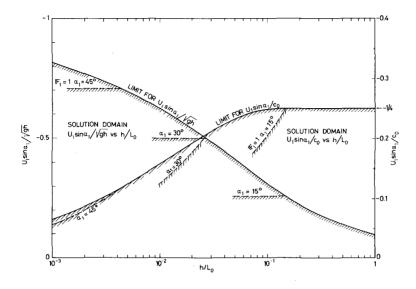
Fig 3. Solution domains for region 1, corresponding to the com-
       ponent $c_{ga\alpha 1}$ in the orthogonal direction of the absolute
       group velocity being positive (below full curves), or the
       Froude number $\mathbb{F}_1$ being smaller than one (below dotted
       curves).

(2.8) of the absolute group velocity c_{ga} is negative. So <u>in the limit</u>
$c_{ga\alpha} = 0$ <u>the ray goes in the wave front direction,</u> and we have from (2.8)

$$c_{ga\alpha 1} = c_{gr1} + U_1 \sin \alpha_1 = 0 \qquad (4.1)$$

We further have from (3.10) in the above reference

$$\left(\frac{h}{L_o}\right)_{lim} = \frac{(1 - G_1)^2}{8\pi} k_1 h \tanh k_1 h \qquad (4.2)$$

Combining this with (4.1) gives

$$\left(\frac{U_1 \sin\alpha_1}{c_o}\right)_{lim} = - \frac{1 - G_1^2}{4} \tanh k_1 h \qquad (4.3)$$

(Equation (4.1) is in fact a consequence of (4.2) and (3.4).) Equations
(4.2) and (4.3) are the bases of the limiting curves in Fig 3. In the
limit we attain minimum values of L, see Jonsson et al (1971). (Note: In
that reference $c_{ga\alpha}$ was for brevity denoted c_{ga}. This is unfortunate,
since c_{ga} should be reserved for the magnitude $|\vec{c}_{ga}|$ of the absolute
group velocity. So in this study we have from Fig 1 $c_{ga\alpha} = c_{ga} \cos(\mu - \alpha)$.)
In deep water we find the well-known limit $U_1 \sin\alpha_1/c_o = -1/4$.

   In Fig 3 we have also shown $(U_1 \sin\alpha_1/\sqrt{gh})_{lim}$ versus h/L_o. For the
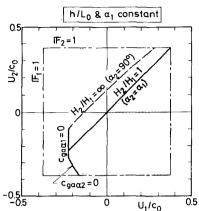latter going towards zero, the former goes towards $-1+$. It is seen, ge-

Fig 4. Solution domains for re-
gion 2, corresponding to
L_2/L_0-figures. Schema-
tical.

Fig 5. Solution domains for re-
gion 2, corresponding to
α_2- and H_2/H_1-figures.
Schematical.

nerally, that if we restrict ourselves to consider Froude numbers $\mathbb{F}_1$ (de-
fined as $|U_1|/\sqrt{gh}$) smaller than one, then this requirement can be 'stric-
ter' than the limiting curve in Fig 3, especially so for the smaller α_1-
values. Also for the $U_1 \sin\alpha_1/c_0$ solution domain, some $\mathbb{F}_1 = 1$ limits are
sketched.

To sum up, the full curves in Fig 3 both correspond to (a) wave rays
being orthogonal to wave orthogonals and (b) wave lengths attaining their
minimum value. The dotted curves correspond to $\mathbb{F}_1 \equiv |U_1|/\sqrt{gh} = 1$, for
different angles of incidence.

The position of the limit $c_{ga\alpha1} = 0$ is sketched in Fig 4 (L_2/L_0 solu-
tions) and Fig 5 (H_2/H_1 and α_2 solutions). It naturally corresponds to
negative U_1-values. In these figures also the $\mathbb{F}_1 = 1$ (and $\mathbb{F}_2 = 1$) limits
are shown. In Fig 4 the position of the (chosen) $\mathbb{F} = 1$ limits depend on
α_1. Note also in this figure that with the requirement $\mathbb{F} < 1$, there are
never solutions outside the "$\mathbb{F} = 1; \alpha_1 = 90°$ frame". The limits can be
recognized in the figures in Chapter 5. It appears from these that the
mutual positions of the limiting curves in Figs 4 and 5 are not absolute.
Thus the $\mathbb{F} = 1$ curves in Fig 5 can lie outside the chosen $U_1/c_0 - U_2/c_0$
frame. And the $c_{ga\alpha1} = 0$ limit can lie to the left of the $\mathbb{F} = 1$ limit.

REGION 2 – In this region there is one further restriction on the input
parameters: The wave height H_2 must remain finite, corresponding to $\alpha_2 <
90°$. Thus there are restrictions on the current strength, whether nega-
tive or positive. In the former case, one obvious condition is the same
as that in region 1, that $c_{ga\alpha}$ be positive. In this limit we thus have
from (2.8)

$$c_{ga\alpha2} = c_{gr2} + U_2 \sin\alpha_2 = 0 \qquad\qquad (4.4)$$

stating that the ray goes in the direction of the wave front. So (4.2) and (4.3), and Fig 3, are also valid with subscripts 2. Fig 3 is not directly applicable, however, since α_2 is not known beforehand. The position of the limit $c_{ga\alpha2} = 0$ is sketched in Figs 4 and 5, and can be found again in the figures in Chapter 5.

It should be observed that – in contrast to plane shoaling, see Jonsson et al (1971) – minimum wave length here does <u>not</u> correspond to infinite wave height. This is because in out case $c_{ga\alpha2} = 0$ (⇒ $L_{2,min}$) does not yield $c_{ga2} = 0$. (Moreover, c_{ga2} can never vanish here.) If, however, U_2 is much larger than U_1, the waves cannot "penetrate" through the shear layer, and H_2/H_1 tends to infinity. This case was already discussed in Chapter 3, and it corresponds to $\mu_2 = 90^o$, giving ray separation factor $\beta_r = 0$. Fig 2 shows that here we must also have $\alpha_2 = 90^o$, which is in accordance with (3.14).

The corresponding limiting curves are depicted in Figs 4 and 5, and can be found again in the figures in Chapter 5. Note that in Fig 4 the position is a function of α_1. The $\alpha_1 = 0^o$ limit is peculiar, since it also corresponds to $L_2/L_o \to \infty$.

In <u>shallow water</u> the $\alpha_2 = 90^o$ limit corresponds to

$$\frac{U_2 - U_1}{c_o} = \frac{1 - \sin\alpha_1}{\sin\alpha_1} \sqrt{\frac{2\pi h}{L_o}} \qquad \text{or} \qquad \frac{U_2 - U_1}{\sqrt{gh}} = \frac{1 - \sin\alpha_1}{\sin\alpha_1} \qquad (4.5)$$
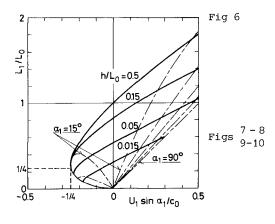
So here, where there is no dispersion, the critical condition – for a fixed value of α_1 – only depends on the current velocity <u>difference</u>.

In the figures, also the limits corresponding to $\mathbb{F}_2 \equiv |U_2|/\sqrt{gh} = 1$ are shown.
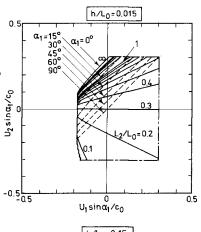

5.   NUMERICAL RESULTS

WAVE LENGTHS L_1/L_o – Solutions to (3.4) are presented in Fig 6, which clearly demonstrates the "stretching" effect of a positive current, and the "compressive" effect of a negative ditto. Other things being equal, wave length increases with increasing current velocity and depth. The deep water limit ($U_1 \sin\alpha_1/c_o$, L_1/L_o) = (-1/4 , 1/4) is clearly seen. The thin full curve connecting this point with origo corresponds to – for every fixed value of h/L_o – the minimum value of L_1/L_o (i e $c_{ga\alpha1} = 0$). To every angle of incidence the $\mathbb{F} = 1$ limit yields two curves – the solution domain lies between these. The solution domains were also illustrated in Fig 3.
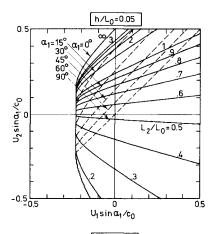

WAVE LENGTHS L_2/L_o – Solutions to (3.8) are presented in Figs 7 - 10, corresponding to four dimensionless water depths h/L_o. Note that $\sin\alpha_1$ – not $\sin\alpha_2$ – appears together with U_2 on the ordinate axis. It is seen that other things being equal, wave length in region 2 increases with increasing current velocity, as expected. The variation of L_2 with U_2 gets slower as U_1 grows. As to the solution limit, we can inspect Fig 7; starting at the bottom and going anti-clockwise the limits correspond to:
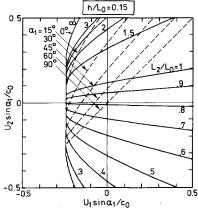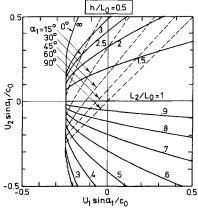
Fig 6   Dimensionless wave length L_1/L_O in region 1 vs $U_1\sin\alpha_1/c_O$ for $h/L_O = 0.015$, 0.05, 0.15, and 0.5. For $U_1\sin\alpha_1 < 0$ the two dot-and-dash lines correspond to $\mathbb{F}_1 = 1$ for $\alpha_1 = 15°$ and $30°$. For $U_1\sin\alpha_1 > 0$ the five dot-and-dash lines correspond to $\mathbb{F}_1 = 1$ for $\alpha_1 = 15°$, $30°$, $45°$, $60°$, and $90°$.

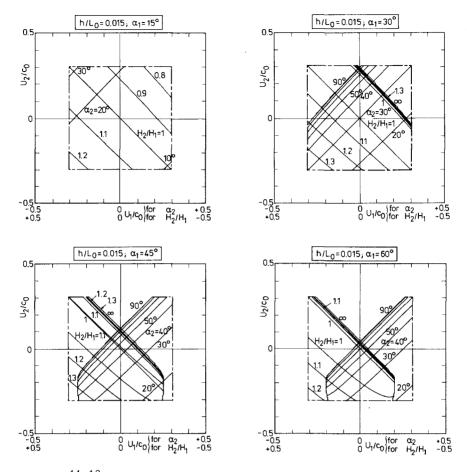Figs $\begin{matrix} 7 - 8 \\ 9-10 \end{matrix}$ Contours for dimensionless wave length L_2/L_O in region 2 vs $U_1\sin\alpha_1/c_O$ and $U_2\sin\alpha_1/c_O$. For $L_2/L_O \leq 1$ the contours are plotted with intervals of 0.1. For $1 \leq L_2/L_O \leq 3$ the contours are plotted with intervals of 0.5. Dot-and-dash lines correspond to $\mathbb{F} = 1$. Dotted curves correspond to $H_2/H_1 = \infty$.
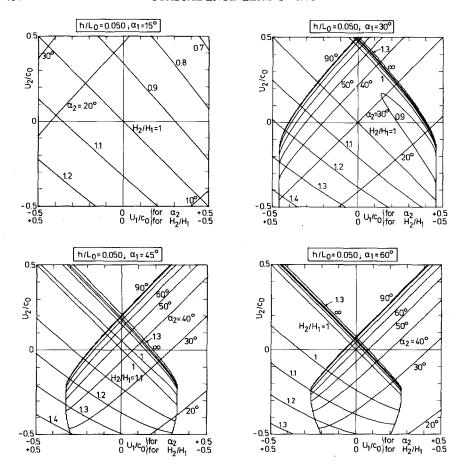
Contours for refraction angle α_2 and relative wave
height H_2/H_1 in region 2 vs U_1/c_0 and U_2/c_0. For α_2
the contours are plotted with intervals of $10°$. For
$H_2/H_1 \leq 1.3$ the contours are plotted with intervals
of 0.1. Dot-and-dash lines correspond to $\mathbb{F} = 1$. Note
that the abscissa axis is reversed for H_2/H_1.

$\mathbb{F}_2 = 1$, $\mathbb{F}_1 = 1$, $\mathbb{F}_2 = 1$, $H_2/H_1 = \infty$, $c_{ga\alpha 1} = 0$, and $c_{ga\alpha 2} = 0$. For details see
Chapter 4 and Fig 4. In Figs 8 - 10 the $\mathbb{F} = 1$ limits lie outside the chosen
frame. Some of the limiting curves appear jagged because of the discreti-
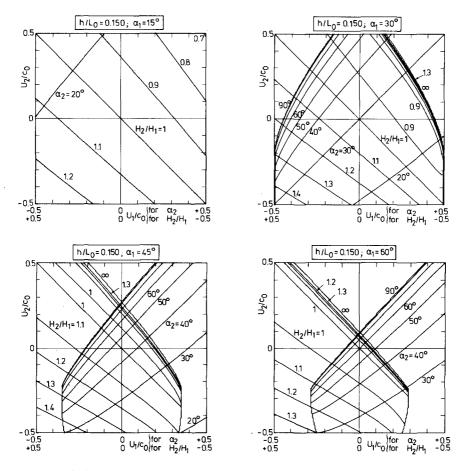zation used in the computer software, which was used to plot these curves.

REFRACTION ANGLES α_2 - Solutions to (3.9) are presented in Figs 11 - 26,
corresponding to four water depths (same as for L_2/L_0), and four angles
of incidence. (H_2/H_1 is shown laterally reversed in the same figures). It
appears that the variation of α_2 is slowest for the smallest angle of in-

Figs 15-16 17-18   Contours for refraction angle α_2 and relative wave height H_2/H_1 in region 2 vs U_1/c_0 and U_2/c_0. For α_2 the contours are plotted with intervals of $10°$. For H_2/H_1 the contours are plotted with intervals of 0.1 up to 1.3 above the diagonal, and 1.4 below it.

cidence α_1 chosen. Everywhere α_2 increases with increasing U_2. It can also be seen that (naturally) for $U_2 = U_1$ we have $\alpha_2 = \alpha_1$. Only for the smallest water depth, the $\mathbb{F} = 1$ limits lie within the chosen frame. The other limits are discussed in Chapter 4 and illustrated in Fig 5.
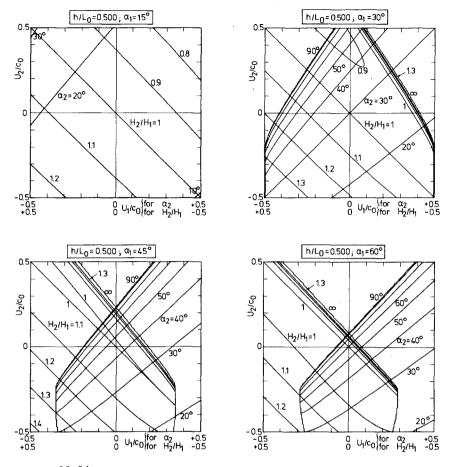

WAVE HEIGHTS H_2/H_1 - Solutions to (3.14) are presented (laterally reversed) in Figs 11 - 26, for four water depths and four angles of incidence. It appears that the variation of H_2/H_1 is slowest for the smallest angle of incidence α_1 chosen. It is also seen that - except for this value of α_1 - the variation with U_2 exhibits a minimum for H_2/H_1 within the chosen

Figs 19-20 21-22 Contours for refraction angle α_2 and relative wave height H_2/H_1 in region 2 vs U_1/c_o and U_2/c_o. For α_2 the contours are plotted with intervals of 10°. For H_2/H_1 the contours are plotted with intervals of 0.1 up to 1.3 above the diagonal, and 1.4 below it.

frame. This will be discussed later. For $U_2 = U_1$ we have $H_2 = H_1$. The limits are discussed in Chapter 4 and illustrated in Fig 5.

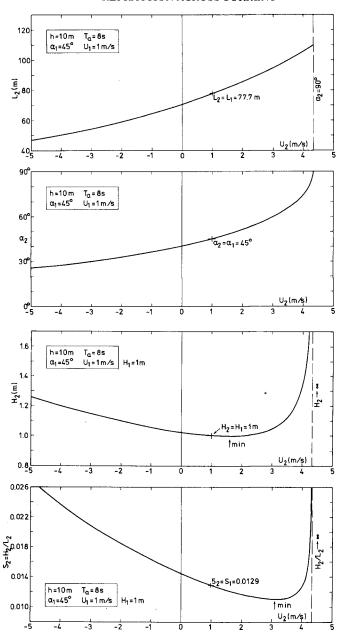VARIATIONS OF L_2, α_2, H_2, S_2, and S_2/S_1 - A physical discussion of the transforming effect of the shear layer is facilitated by looking at a few concrete examples. Consider first the sequence in Figs 27 - 30, giving the variation of region 2 quantities with U_2. Fig 27 shows how L_2 increases monotonously with increasing U_2; the maximum value is attained for $\alpha_2 = 90^\circ$. Also α_2 (Fig 28) varies in this way; for $U_2 > 4.3$ m/s (approx) $\alpha_2 = 90^\circ$, and waves cannot penetrate into region 2. In the limit H_2 theoreti-
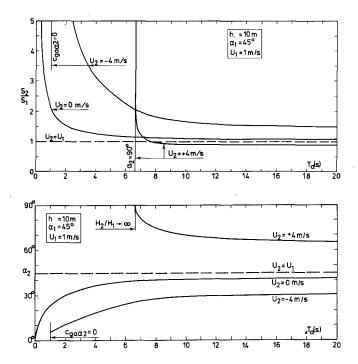
Figs 23-24 25-26   Contours for refraction angle α_2 and relative wave height H_2/H_1 in region 2 vs U_1/c_0 and U_2/c_0. For α_2 the contours are plotted with intervals of $10°$. For H_2/H_1 the contours are plotted with intervals of 0.1 up to 1.3 above the diagonal, and 1.4 below it.

cally tends to infinity (Fig 29). It is also seen from this figure that H_2 has a minimum. This can be anticipated by looking at (3.12); H_2 can become large, if c_{ga} becomes small (Fig 29, left), or if ray width e (see Fig 2) becomes small (Fig 29, right), so a minimum in between is expected. Fig 30 shows that the wave steepness S_2 has a sharper minimum. This is because L_2 is decreasing as U_2 decreases. The figure shows that both a large negative <u>and</u> a large positive current can have a strong steepening effect on the wave; eventually it may break.

The influence of the (absolute) period is illustrated in Fig 31, which gives the ratio between steepnesses in regions 2 and 1. It appears that

Figs 27-30 Wave length L_2 (Fig 27), refraction angle α_2 (Fig 28), wave height H_2 (Fig 29), and wave steepness $S_2 \equiv H_2/L_2$ (Fig 30) vs current velocity U_2 for fixed values of water depth h, absolute wave period T_a, angle of incidence α_1, current velocity U_1, and wave height H_1 (Figs 29-30).

Figs 31-32   Relative wave steepness $S_2/S_1 \equiv (H_2/L_2)/(H_1/L_1)$
             (Fig 31) and refraction angle α_2 (Fig 32) vs ab-
             solute wave period T_a for fixed values of water
             depth h, angle of incidence α_1, and current velo-
             city U_1.

both a large negative <u>and</u> a large positive current have a dramatic steep-
ening effect on waves of smaller period, either because the group speed
and wave length become small (opposing current), or because the ray sepa-
ration factor becomes small (following current), opposing current here
meaning $U_2 - U_1 < 0$. In both cases the effect is due to the fact that
"short waves are slow waves". This steepening and thus filtering effect
was illustrated by Isaacs (1948); in the photo in his Fig 1 the current
discontinuity shows up as a foam line because of short wave breaking.
Fig 31 also shows that the steepness ratio is remarkably constant for the
higher periods.

   The period influence on the refraction angle is shown in Fig 32. For
$U_2 = +4$ m/s the variation towards $\alpha_2 = 90^{\circ}$ as T_a tends to 6.6 s (approx),
reflects that here the ray separation factor goes towards zero.

   Finally the influence of the (constant) water depth on S_2/S_1 is shown
in Fig 33. It appears that (naturally) the effect is largest on smaller
depths, because other things being equal here the phase speed is smallest.
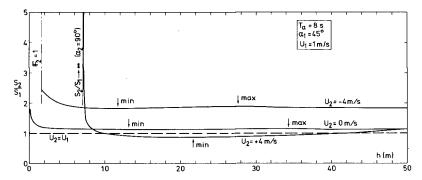For h > 10 m the variation is quite small in the case considered.

Fig 33   Relative wave steepness $S_2/S_1 \equiv (H_2/L_2)/(H_1/L_1)$ vs water
depth h for fixed values of absolute wave period T_a,
angle of incidence α_1, and current velocity U_1.

EXAMPLE - It can be difficult to read the quantities in the dimensionless
delineations in Figs 6 - 26 with any great accuracy (also a number of in-
terpolations are necessary). These figures illustrate the trends, but can
give only approximate values. It is not altogether difficult, however, to
find the exact figures by calculation. This will be demonstrated in the
following. Consider the case with h = 10 m, T_a = 8 s, α_1 = 45°, U_1 = 1 m/s,
U_2 = -2 m/s, and H_1 = 1 m (Figs 27 - 30). (g = 9.80665 m/s^2 ⇒ g/2π ≈ 1.561 m/s^2).
Calculation of L_1 - c_0 = 1.561·8 = 12.49 m/s, L_0 = 1.561·8^2 = 99.90 m ⇒ h/L_0 =
0.1001; q* = 10·1·sin 45°/(12.49·99.90) = 0.00567. Table 6-a in Jonsson et
al (1971) (or Table 3.2-I in Jonsson, 1978b) then gives L/L_0 = 0.778 ⇒ L_1 =
0.778·99.90 = 77.7 m. (Without a current we find L = 70.9 m - the wave is
"stretched" by the positive current.)
Calculation of L_2 - The right hand side of (3.8) squared is 0.1001(1-(-2)·
sin 45°·8/77.7)^2 = 0.1314. Using this as entry in the column "h/L_0" in a
conventional wave table, we find h/L = 0.1677 ⇒ L_2 = 10/0.1677 = 59.6 m, which
agrees with Fig 27. (The wave is "compressed" in region 2 by the opposing
current).
Calculation of α_2 - From (3.9) we find α_2 = Arcsin(59.6 sin 45°/77.7) =
32.°8, which agrees with Fig 28.
Calculation of H_2 - h/L_1 = 10/77.7 = 0.1287; h/L_2 = 0.1677. From a conven-
tional wave table we then find G_1 = 0.6682 and G_2 = 0.5200. Then from (3.14)
H_2 = 1·$\sqrt{1.6682/1.5200}$·$\sqrt{\sin 90°/\sin 65.°6}$ = 1.098 m, which agrees with Fig 29.
($S_2 \equiv H_2/L_2$ = 1.098/59.6 = 0.0184, which agrees with Fig 30).

6.   CONCLUSIONS

    Analytical expressions are presented for the determination of wave
length L_2 (3.8), refraction angle α_2 (3.9), and wave height H_2 (3.14), as
a wave passes a large-scale shearing current over a horizontal bed. The
current velocity is assumed constant in time and over depth. Dimensionless
results are presented in Figs 7 - 10 (L_2) and 11 - 26 (α_2 and H_2). The di-
rect effect of the current velocity U_2 in region 2 (see Fig 1) is illustra-
ted in a concrete example in Figs 27 - 30. The most interesting feature
here is the display of a wave height (and steepness) minimum. The "filter-
ing" effect of a shear layer on a wave motion is illustrated in Figs 31
and 32, and the influence of the water depth on wave steepness change ap-
pears from Fig 33.

The wave length L_1 at the initial state (region 1, see Fig 1) is determined by (3.4); solutions in dimensionless form are illustrated in Fig 6. Solution domains for region 1 appear from Fig 3. Solution domains for region 2 are sketched in Figs 4 (applicable to L_2-figures) and 5 (applicable to α_2- and H_2-figures).

A detailed example of how to obtain numerical results using tables and handcalculations, is given in Chapter 5.

APPENDIX: ORTHOGONALS AND RAYS

In the general case the wave <u>orthogonals</u> are determined by

$$Dx/Ds = \cos A \qquad (A.1) \qquad Dy/Ds = \sin A \qquad (A.2)$$

$$DA/Ds = (\sin A \, \partial c_a/\partial x - \cos A \, \partial c_a/\partial y)/c_a \qquad (A.3)$$

in which x and y are horizontal Cartesian coordinates, s is distance along the orthogonal, A is the angle from the x-axis to the positive direction of the orthogonal (DA/Ds is the orthogonal curvature), and c_a is the absolute phase speed

$$c_a = c_r + u \cos A + v \sin A \qquad (A.4)$$

In (A.4) c_r is the relative phase speed (3.1) and $\vec{U} = (u,v)$ is the current vector. In (A.1) to (A.3) time t can be introduced through $Ds = c_a dt$. Thus <u>formally</u> the wave orthogonal equations are the same as for pure depth refraction, see Skovgaard et al (1975).

In the general case the wave <u>rays</u> are determined by

$$Dx/Dr = \cos \mu \qquad (A.5) \qquad Dy/Dr = \sin \mu \qquad (A.6)$$

$$D\mu/Dr = \cos^2\mu \, D(\tan \mu)/Dr \qquad (A.7)$$

in which r is distance along the ray and μ is the angle from the x-axis to the positive direction of the ray determined by

$$\tan \mu = (c_{gr} \sin A + v)/(c_{gr} \cos A + u) \qquad (A.8)$$

In (A.8) c_{gr} is the relative group speed (3.2). Note that according to (A.8) $\mu = A$ for $(u,v) = (0,0)$; however, (A.7) does not transform to (A.3) in this limit. This is because (A.7) presupposes (A.3) to be known and solved, giving angle A. (The ray separation factor is determined by (31) in Skovgaard and Jonsson, 1977).

REFERENCES

Christoffersen, J.B., and I.G. Jonsson, 'A note on wave action conservation in a dissipative medium', manuscript submitted for publication, 1979.

Evans, D.E., 'The transmission of deep-water waves across a vortex sheet', J. Fluid Mech., 68, 389-401, 1975.

Isaacs, J.D., Discussion of 'Refraction of surface waves by currents' by J.W. Johnson. Trans.Am.Geophys.Un., 29, 739-742, 1948.

Jonsson, I.G., 'The dynamics of waves on currents over a weakly varying bed', in 'Waves on Water of Variable Depth', eds. D.G. Provis and R. Radok. Lecture Notes in Physics, 64, 133-144, Springer-Verlag, Berlin, 1977.

Jonsson, I.G., 'Energy flux and wave action in gravity waves propagating
    on a current', J. Hydr.Res., 16, 223-234, 1978 a.
Jonsson, I.G., 'Combinations of waves and currents', in 'Stability of Ti-
    dal Inlets' by Per Bruun, 162-203. Elsevier, Amsterdam, 1978 b .
Jonsson, I.G., and J.D. Wang, 'Current depth refraction of water waves',
    Inst.Hydrodyn. and Hydraulic Engng. (ISVA), Series Paper No.18, 48 pp.,
    1978.
Jonsson, I.G., O. Brink-Kjær, and G.P. Thomas, 'Wave action and set-down
    for waves on a shear current', J. Fluid Mech., 87, 401-416, 1978.
Jonsson, I.G., C. Skougaard, and J.D. Wang, 'Interaction between waves and
    currents', Proc. 12th Coastal Engng. Conf., Wash., D.C., Sep. 1970. Am.
    Soc.Civ.Engrs., New York, 1, 489-507, 1971.
Longuet-Higgins, M.S., and R.W. Stewart, 'The changes in amplitude of
    short gravity waves on steady non-uniform currents', J. Fluid Mech.,
    10, 529-549, 1961.
Peregrine, D.H., 'Interaction of water waves and currents', in 'Advances
    in Applied Mechanics', ed. C.-S. Yih, Academic Press, New York, 16,
    9-117, 1976.
Savitsky, D., 'Interaction between gravity waves and finite turbulent
    flow fields', Proc. 8th Symp. on Naval Hydrodyn., 389-446, Arlington,
    Virginia: Office of Naval Research, 1970.
Skovgaard, O., and I.G.Jonsson, 'Current depth refraction using finite
    elements', Proc. 15th Coastal Engng. Conf., Honululu, Hawaii, July 1976.
    Am.Soc.Civ.Engrs., New York, 1, 721-737, 1977.
Skovgaard, O., I.G. Jonsson, and J.A. Bertelsen, 'Computation of wave
    heights due to refraction and friction', J. Waterways, Harbors and
    Coastal Engrg. Div., Am.Soc.Civ.Engrs., New York, 101, WW1, 15-32,
    1975 + closure: 102, WW1 , 100-105, 1976.
Wiegel, R.L.,'Oceanographical Engineering', Prentice-Hall, Inc., Englewood
    Cliffs, N.J., 1964.